The Kinematics of Conical Involute Gear Hobbing

Carlo Innocenti

(This article first appeared in the proceedings of IMECE2007, the 2007 ASME International Mechanical Engineering Congress and Exposition, November 11–15, 2007, Seattle, Washington, USA. It is reprinted here with permission.)

Management Summary

It is the intent of this presentation to determine all rigid-body positions of two conical involutes that mesh together, with no backlash. That information then serves to provide a simple, general approach in arriving at two key setting parameters for a hobbing machine when cutting a conical (beveloid) gear. A numerical example will show application of the presented results in a case study scenario. Conical involute gears are commonly seen in gearboxes for medium-size marine applications—onboard engines with horizontal crankshafts and slightly sloped propeller axes—and in automatic packaging applications to connect shafts with concurrent axes whenever the angle between these axes is very small (a few degrees).

Introduction

Conical involute gears, also known as beveloid gears, are generalized involute gears that have the two flanks of the same tooth characterized by different base cylinder radii and different base helix angles (Refs. 1– 4). Beveloid gears can be mounted on parallel-, intersecting- or skew-axis shafts. They can be cheaply manufactured by resorting to the same cutting machines and tools employed to generate conventional, involute helical gears. The only critical aspect of a beveloid gear pair, i.e., the theoretical punctiform (single-point) contact between the flanks of meshing gears, can be offset by a careful choice of the geometric parameters of a gear pair (Refs. 5–7). On the other hand, the localized contact between beveloid gear teeth comes in handy should the shaft axes be subject to a moderate, relative position change in assembly or operation.

The technical literature contains plenty of information regarding the tooth flank geometry (Refs. 8–9) and the setting of a hobbing machine in order to generate a beveloid gear (Refs. 10–15). Unfortunately, the formalism usually adopted makes determination of the hobbing parameters a rather involved process, mainly because the geometry of a beveloid gear is customarily—though inefficiently—specified by resorting to the relative placement of the gear with respect to the standard rack cutter that would generate the gear, even if the gear is to be generated by a different cutting tool. To make things worse, some of the cited papers on beveloid gear hobbing are hard reading due to printing errors in formulae and figures.

This paper presents an original method to compute the parameters that define the relative movement of a hob with respect to the beveloid gear being generated. Pivotal to the proposed method, together with a straightforward description of a beveloid gear in terms of its basic geometric features, is the determination of the set or relative rigid-body positions of two tightly meshing beveloid gears. Based on this set of relative positions, the paper shows how to assess the rate of change of the hob-work shaft axis distance as the hob is fed across the work, as well as the rate of the additional rotation of the hob relative to the gear. These parameters have to be entered into the controller of a CNC hobbing machine in order to generate a given beveloid gear.

The proposed method also can be applied to the grinding of beveloid gears by the continuous generating grinding process. Furthermore, it can be extended to encompass the cases of swivel angle modification and hob shifting during hobbing.

Lines of Contact

The hob that generates a beveloid gear in a hobbing machining process can be considered an involute gear. Most commonly, such a gear is of the cylindrical type, although adoption of a conical involute hob would be possible too, in principle. For this reason, the kinematics of hobbing will be presented in this paper by referring to a beveloid hob, and subsequently specialized to the case of a cylindrical hob.

This section introduces the nomenclature adopted in the paper and summarizes known results pertaining to the loci of contact of a conical involute gear set. The reader is referred to References 16 and 17 for a detailed explanation of the reported concepts and formulas.

The tooth flanks of a conical involute gear are portions of involute helicoids. As opposed to classical helical involute gears, the two helicoids of the same tooth of a conical involute gear do not generally stem from the same base cylinder, nor have the same lead.

In a beveloid gear set composed of gears G_1 and G_2, the axis of gear G_1 is here directed in either way by unit vector $\boldsymbol{n}_1$. The orientation of the axis of gear G_2 by unit vector $\boldsymbol{n}_2$ is then so chosen as to make the right-hand flanks of gear G_1 come into contact with the right-hand flanks of gear G_2. With reference to Figure 1, the distinction between right-hand and left-hand tooth flanks is possible based on the sign of the ensuing quantity:

$$\boldsymbol{q}_i \times (F_i - O_i) \cdot \boldsymbol{n}_i \qquad (1)$$

where F_i is a point on a tooth flank of gear G_i (i=1, 2), O_i is a point on the axis of gear G_i, and $\boldsymbol{q}_i$ is the outward-pointing unit vector perpendicular to the tooth flank at F_i. A tooth flank is a right-hand or left-hand flank, depending on whether Equation 1 results in a positive or, respectively, negative quantity. (In Figure 1, point F_i lies on a right-hand flank of gear G_i). In the sequel, index j will be systematically used to refer to right-hand ($j = +1$) or left-hand ($j = -1$) tooth flanks.

The basic geometry of gear G_i (i=1, 2) is defined by its number of teeth N_i, the radii $\rho_{i,j}$ ($j = \pm 1$) of its base cylinders, the base helix angles $\beta_{i,j}$ of its involute helicoids ($|\beta_{i,j}| < \pi/2$; $\beta_{i,j} > 0$ for right-handed helicoids), and the base angular thickness φ'_i of its teeth at a specified cross section. All these parameters—with the exception of N_i—are reported in Figure 1, which also shows the involute helicoids as stretching inwards up to their base cylinders, irrespective of their actual radial extent.

The normal base pitch is the distance between homologous involute helicoids of adjacent teeth of the same gear. A beveloid gear has two normal base pitches—$p_{i,1}$ and $p_{i,-1}$—one for right-hand flanks and one for left-hand flanks. Their expression is:

$$p_{i,j} = \frac{2\pi\rho_{i,j}\,u_{i,j}}{N_i} \qquad (i = 1,2;\ j = \pm 1) \qquad (2)$$

where

$$u_{i,j} = \cos\beta_{i,j} \qquad (i = 1,2;\ j = \pm 1) \qquad (3)$$

Two beveloid gears can mesh only if they have the same normal base pitches, i.e., only if the ensuing conditions are satisfied:

$$\begin{cases} p_{1,1} = p_{2,1} \\ p_{1,-1} = p_{2,-1} \end{cases} \qquad (4)$$

Owing to Equation 4, the following equations and ensuing text and figures will refer to the normal base pitch of right-hand and left-hand flanks of both gears as p_1 and p_{-1} respectively.

The common perpendicular to the axes of a pair of meshing beveloid gears intersects the axes themselves at points A_1 and A_2 (Fig. 2). The relative position of these axes

continued

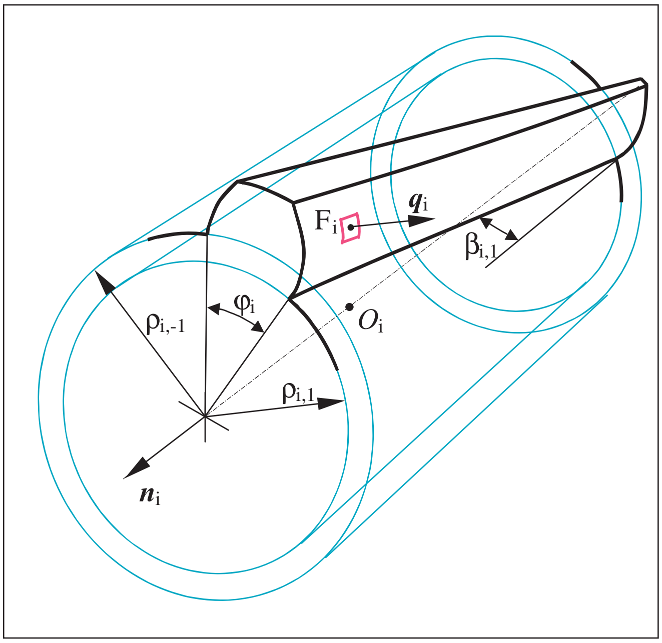

Figure 1—Basic dimensions of beveloid gear G_i.

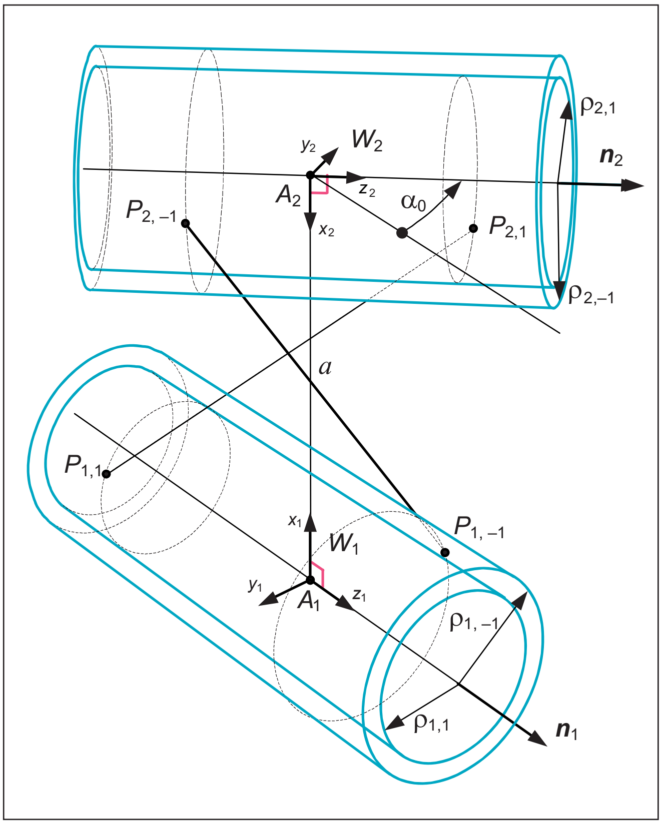

Figure 2—The lines of contact.

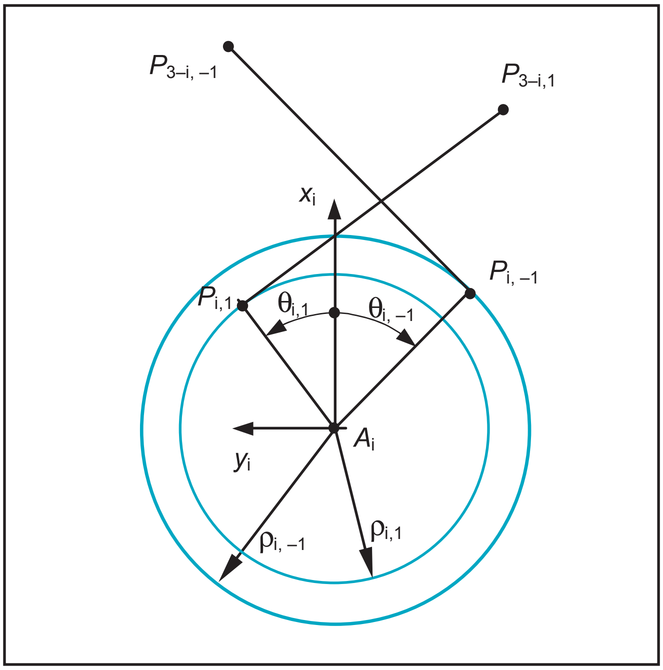

Figure 3—Coordinates of the extremities of the lines of contact.

is defined by their mutual distance a_0, together with their relative inclination α_0. Specifically, angle α_0 is the amplitude of the virtual rotation—positive if counterclockwise—about vector $(A_2–A_1)$ that would make unit vector $\boldsymbol{n}_1$ align with unit vector $\boldsymbol{n}_2$. Two fixed Cartesian reference frames W_i (i =1, 2) are then introduced with origins at points A_i, x_i axis pointing towards A_{3-i}, and z_i axis directed as unit vector $\boldsymbol{n}_i$.

For a conventional beveloid gear set composed of two meshing conical involute gears that revolve about their fixed and non-parallel axes, the locus of possible points of contact between the involute helicoids of right-hand (left-hand) flanks is a line segment that has a definite position with respect to either of reference frames W_i (i=1, 2). More specifically, the line of contact is tangent at its ending points $P_{1,1}$ and $P_{2,1}$ ($P_{1,-1}$ and $P_{2,-1}$) to the base cylinders of the right-hand (left-hand) flanks of the two gears. This is true even if the actual tooth flanks—being limited portions of the above-mentioned involute helicoids—touch each other along line segments that are shorter than the above-mentioned lines of contact and superimposed on them.

The cosine and sine of the angle $\theta_{i,j}$ that the projection of vector $(P_{i,j} – A_i)$ on the xy-plane of reference frame W_i forms with the x-axis of W_i (see Fig. 3) are indirectly provided by:

$$c_{i,j} = -\frac{v_{h,j} + u_0 v_{i,j}}{v_0 u_{i,j}} \qquad (i = 1,2;\ h = 3-i;\ j = \pm 1) \tag{5}$$

$$s_{i,j} = \lambda_j \frac{\sqrt{Q_j}}{v_0 u_{i,j}} \qquad (i = 1,2;\ j = \pm 1) \tag{6}$$

where

$$c_{i,j} = \cos\theta_{i,j}; \qquad s_{i,j} = \sin\theta_{i,j} \qquad (i = 1,2;\ j = \pm 1) \tag{7}$$

$$v_{i,j} = \sin\beta_{i,j} \qquad (i = 1,2;\ j = \pm 1) \tag{8}$$

$$u_0 = \cos\alpha_0; \qquad v_0 = \sin\alpha_0 \tag{9}$$

$$\lambda_j = j\,\mathrm{sign}\left[v_0\left(a_0 - \rho_{1,j}c_{1,j} - \rho_{2,j}c_{2,j}\right)\right] \qquad (j = \pm 1) \tag{10}$$

$$Q_j = v_0^2 - v_{1,j}^2 - v_{2,j}^2 - 2u_0 v_{1,j} v_{2,j} \qquad (j = \pm 1) \tag{11}$$

The function sign(.) in Equation 10 returns the value + 1, 0, or –1 depending on whether its argument is positive, zero or negative. In Figure 3, angle $\theta_{i,1}$ is positive, whereas angle $\theta_{i,-1}$ is negative.

Due to the square root in Equation 6, two beveloid gears can properly mesh only if condition

$$Q_j \geq 0 \qquad (j = \pm 1) \tag{12}$$

is satisfied for both values of j. In the following equations, text and figures Equation 12 will be supposed as holding.

Thanks to Equations 5 and 6, angle $\theta_{i,j}$ can be expressed as:

$$\theta_{i,j} = 2\lambda_j \arctan\frac{v_0 u_{i,j} + u_0 v_{i,j} + v_{h,j}}{\sqrt{Q_j}} \tag{13}$$

(i=1,2; h= 3 – i; j= ± 1).

The z-coordinate $b_{i,j}$ of point $P_{i,j}$ in reference frame W_i (i=1,2; j= ± 1) is given by:

$b_{1,j}$=

$$-\lambda_j \frac{a_0 u_{h,j}\left(v_{i,j} + u_0 v_{h,j}\right) + \rho_{i,j} v_0\left(u_0 + v_{i,j} v_{h,j}\right) + \rho_{h,j} v_0 u_{i,j} u_{h,j}}{v_0 u_{i,j}\sqrt{Q_j}} \tag{14}$$

Based on the relative positions of reference frames W_1 and W_2, together with the cylindrical coordinates $\rho_{i,j}$, $\theta_{i,j}$, and $b_{i,j}$ of points $P_{i,j}$ with respect to W_i (i=1,2; j= ± 1), the length σ_j of the line of contact $P_{1,j}P_{2,j}$ can be determined by (Refs. 16–17):

$$\sigma_j = j\lambda_j v_0 \frac{a_0 - \rho_{1,j}c_{1,j} - \rho_{2,j}c_{2,j}}{\sqrt{Q_j}} \qquad (j = \pm 1) \tag{15}$$

The results summarized so far are directly applicable to a conventional beveloid gear set, i.e., to a pair of meshing beveloid gears that revolve about their rigidly connected axes. They also represent a convenient starting point for determining all possible relative positions of a beveloid hob relative to the beveloid gear being machined.

A Backlash-Free Beveloid Gear Set

Due to the single-point contact between tooth flanks of a beveloid gear set, the assortment of rigid-body positions of a beveloid hob relative to the beveloid gear being machined cannot be confined to the simple infinity of relative positions of two gears in a conventional beveloid gear set. Otherwise, a gear machined by a beveloid hob would not have involute helicoidal flanks; rather, only one curve on these flanks would belong to the desired involute helicoids.

Therefore the double infinity of points on a tooth flank of a beveloid gear machined by a beveloid hob has to be obtained at least as a two-parameter envelope of the positions of the hob tooth flanks. Each of these positions must correspond to a meshing configuration—with no backlash—of the beveloid hob with the finished beveloid gear.

There is a quadruple infinity of configurations of a beveloid gear tightly meshing with a beveloid hob (the contacts between right-hand flanks, as well as the contacts between left-hand flanks, each diminish by one the original six degrees of freedom that possess, in principle, a freely-movable hob that does not touch the gear). The double infinity of rigid-body positions of the hob relative to the generated gear is only a subset of the quadruple-infinity possible meshing configurations. This latter set of configurations can be found by first determining the simple infinity of all relative rigid-body positions of two beveloid gears tightly meshing in a conventional gear set, which is just the scope of the present section.

With regards to the same set of beveloid gears considered in the previous section, let φ_{0i} be the common-normal angular base thickness of a tooth of gear G_i (i=1, 2), i.e., the angular base thickness at the cross-section of gear G_i through point A_i (Figs. 1 and 2). On a generic cross-section identified by the axial coordinate z_i, the tooth angular base thickness φ_i' of a tooth of gear G_i is given by

$$\varphi_i' = \varphi_{0i} + \left(k_{i,-1} - k_{i,1}\right) z_i \qquad (i = 1,2) \tag{16}$$

In this equation, quantity $k_{i,j}$ is defined as

$$k_{i,j} = \frac{\tan\beta_{i,j}}{\rho_{i,j}} \qquad (i = 1,2;\ j = \pm 1) \tag{17}$$

Incidentally, $k_{i,j}$ can be given a geometric meaning: If the base helix of an involute helicoid j of gear G_i is projected on the unitary-radius cylinder coaxial with the gear, then the resulting projection is a helix whose inclination angle with respect to the gear axis is $\tan^{-1}k_{i,j}$.

If the surface of the unitary-radius cylinder of gear G_i is now cut along the generator that intersects the negative x-axis of reference frame W_i (Fig. 2), and subsequently flattened (Fig. 4), the former projections of the base helices of a tooth of gear G_i appear as straight lines. In Figure 4, coordinate δ_i—measured from the generator that intersects the positive x-axis of W_i—parameterizes the generators of the unitary-radius cylinder associated with gear G_i. The common-normal angular base tooth thickness φ_{0i} is also shown in Figure 4, together with the point H_i of intersection of the common normal A_1A_2 with the unitary-radius cylinder of gear G_i.

The orientations of gears G_1 and G_2 about their respective axes are defined here by considering an arbitrarily selected reference right-hand flank (involute helicoid) $\Sigma_{1,1}$ on gear G_1, together with the right-hand flank (involute helicoid) $\Sigma_{2,1}$ of the tooth of gear G_2 in contact with $\Sigma_{1,1}$. The reference angular position of gear G_i is chosen here as characterized by helicoid

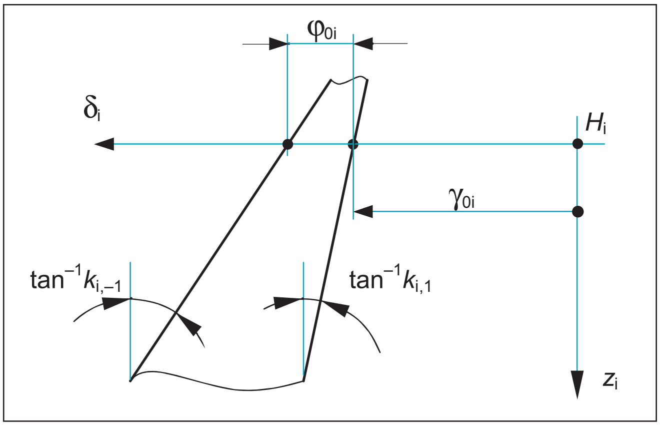

Figure 4—The developed unitary-radius cylinder of gear G_i.

$\Sigma_{i,1}$ intersecting the minimum distance segment A_1A_2 (Fig. 2) at a point of the base cylinder of gear G_i (i=1,2). (Equivalently, at the reference angular position of gear G_i the projection of the base helix of $\Sigma_{i,1}$ on the unitary-radius cylinder of the gear goes through point H_i.) A generic angular position of gear G_i is then identified by the angle γ_{0i} of the rotation that carries the gear from its reference angular position to the considered position. Angle γ_{0i}—positive for a counterclockwise rotation with respect to unit vector $\boldsymbol{n}_i$ (Fig. 2), can also be highlighted on the developed unitary-radius cylinder (Fig. 4).

The angular positions γ_{01} and γ_{02} of two beveloid gears that mesh together with zero backlash are clearly interrelated. An obvious mutual constraint is the differential condition that stems from expressing the gear ratio in terms of the number of teeth N_i (i=1,2) of the two gears

$$\frac{d\gamma_{02}}{d\gamma_{01}} = -\frac{N_1}{N_2} \tag{18}$$

In order to find a finite relation between γ_{01} and γ_{02}, two maneuvers are envisaged. The first maneuver starts with the first gear at position γ_{01}= 0 and—by exploiting the tooth contact between right-hand flanks only—carries the second gear at position γ_{02}= 0. The second maneuver is similar to the first one, but for the reliance on the contact between left-hand flanks.

The first step of the first maneuver consists of making the reference involute helicoid $\Sigma_{1,1}$ of gear G_1 go through the extremity $P_{1,1}$ of the line of contact between helicoids of right-hand flanks (Fig. 2). The corresponding rotation $\Delta\gamma_{01a}$ of gear G_1 is given by

$$\Delta\gamma_{01a} = \theta_{1,1} - k_{1,1}b_{1,1} \tag{19}$$

where $\theta_{1,1}$ and $b_{1,1}$ are provided by Equations 13 and 14, respectively. Equation 19 can be justified by elementary geometric reasoning on the unitary-radius cylinder of gear G_1. (The reader is referred to Reference 16 for further details.)

The second step makes helicoid $\Sigma_{1,1}$ go through point $P_{2,1}$. The necessary rotation of gear G_1 is

continued

$$\Delta\gamma_{01b} = -\frac{2\pi\sigma_1}{N_1\, p_1} \qquad (20)$$

Now helicoids $\Sigma_{1,1}$ and $\Sigma_{2,1}$ touch each other at $P_{2,1}$. By the third—and last—step, gear G_2 is so turned about its axis as to make the base helix of helicoid $\Sigma_{2,1}$ intersect the common normal A_1A_2. The corresponding rotation of gear G_2 is given by

$$\Delta\gamma_{02c} = -\left(\theta_{2,1} - k_{2,1}b_{2,1}\right) \qquad (21)$$

At the end of the considered three-step maneuver, gear G_2 is at its reference position ($\gamma_{02} = 0$), whereas gear G_1 is at a position identified by

$$\Delta\gamma'_{01} = \Delta\gamma_{01a} + \Delta\gamma_{01b} - \frac{N_2}{N_1}\Delta\gamma_{02c} \qquad (22)$$

Owing to Equation 18, and to the existence of a meshing configuration characterized by (γ_{01}, γ_{02}) = ($\Delta\gamma'_{01}$, 0) , the ensuing relation between γ_{01} and γ_{02} must be satisfied

$$N_1\left(\gamma_{01} - \Delta\gamma'_{01}\right) + N_2\gamma_{02} = 0 \qquad (23)$$

Now the second maneuver is taken into account. Its first step consists of bringing gear G_1 from the reference angular position to the position where helicoid $\Sigma_{1,-1}$ goes through point $P_{1,-1}$. Here $\Sigma_{1,-1}$ is the helicoid that, together with the reference helicoid $\Sigma_{1,1}$ defined above, bounds the same tooth of gear G_1. The corresponding rotation of gear G_1 is (see Figs. 2–4):

$$\Delta\gamma_{01d} = -\varphi_{01} + \theta_{1,-1} - k_{1,-1}b_{1,-1} \qquad (24)$$

By the second step, gear G_1 is revolved until helicoid $\Sigma_{1,-1}$ goes through point $P_{2,-1}$. The incremental rotation of gear G_1 is provided by

$$\Delta\gamma_{01e} = \frac{2\pi\sigma_{-1}}{N_1\, p_{-1}} \qquad (25)$$

After this step, the helicoid $\Sigma_{1,-1}$ of gear G_1 touches the helicoid $\Sigma_{2,-1}$ of gear G_2 at point $P_{2,-1}$. It is worth observing that, while $\Sigma_{1,1}$ and $\Sigma_{1,-1}$ bound the same tooth of gear G_1, $\Sigma_{2,1}$ and $\Sigma_{2,-1}$ delimit the same tooth space of gear G_2.

The third step of the current maneuver consists in making helicoid $\Sigma_{2,-1}$ intersect the common normal $A_1\, A_2$ at a point of its base helix. The additional rotation of gear G_2 is provided by

$$\Delta\gamma_{02f} = -\left(\theta_{2,-1} - k_{2,-1}b_{2,-1}\right) \qquad (26)$$

The fourth—and last—step brings gear G_2 at the reference position $\gamma_{02} = 0$, i.e., makes helicoid $\Sigma_{2,1}$ intersect the common normal A_1A_2 at a point of the base helix. The corresponding further rotation of gear G_2 is

$$\Delta\gamma_{02g} = -\frac{2\pi}{N_2} + \varphi_{02} \qquad (27)$$

The angular position of gear G_1 at the end of the whole maneuver is provided by

$$\Delta\gamma''_{01} = \Delta\gamma_{01d} + \Delta\gamma_{01e} - \frac{N_2}{N_1}\left(\Delta\gamma_{02f} + \Delta\gamma_{02g}\right) \qquad (28)$$

Therefore in addition to Equation 23, another constraint between γ_{01} and γ_{02} can be found

$$N_1\left(\gamma_{01} - \Delta\gamma''_{01}\right) + N_2\gamma_{02} = 0 \qquad (29)$$

By considering the expressions of $\Delta\gamma'_{01}$and $\Delta\gamma''_{01}$ provided by Equations 22 and 28, Equations 23 and 29 can be rewritten as

$$N_1\gamma_{01} + N_2\gamma_{02} + B' = 0 \qquad (30)$$

$$N_1\gamma_{01} + N_2\gamma_{02} + B'' = 0 \qquad (31)$$

Quantities B′ and B" that appear in these equations are given by

$$B' = N_1\left(k_{1,1}b_{1,1} - \theta_{1,1}\right) + N_2\left(k_{2,1}b_{2,1} - \theta_{2,1}\right) + \frac{2\pi\sigma_1}{p_1} \qquad (32)$$

$$\begin{aligned} B'' = {} & N_1\left(k_{1,-1}b_{1,-1} - \theta_{1,-1} + \varphi_{01}\right) + \\ & N_2\left(k_{2,-1}b_{2,-1} - \theta_{2,-1} + \varphi_{02}\right) - 2\pi\left(\frac{\sigma_{-1}}{p_{-1}} + 1\right) \end{aligned} \qquad (33)$$

For a given backlash-free beveloid gear set, Equations 30 and 31 must be satisfied simultaneously. Since the considered gear set is a mechanism with one degree of freedom, it should be possible to arbitrarily select γ_{01} (or γ_{02}), and then determine γ_{02} (or γ_{01}). Therefore Equations 30 and 31, when considered as linear equations in γ_{01} and γ_{02}, should be linearly dependent. This requirement translates into the ensuing condition:

$$B' = B'' \qquad (34)$$

By taking into account Equations 32 and 33, Equation 34 can be rewritten as follows (Ref. 16):

$$S_1 + S_2 + T = 0 \qquad (35)$$

where

$$S_i = N_i\left(k_{i,1}b_{i,1} - k_{i,-1}b_{i,-1} - \theta_{i,1} + \theta_{i,-1} - \varphi_{0i}\right) \qquad (i = 1,2) \qquad (36)$$

and

$$T = 2\pi\left(\frac{\sigma_1}{p_1} + \frac{\sigma_{-1}}{p_{-1}} + 1\right) \qquad (37)$$

Equivalent to the equation set composed of Equations 30 and 31, the equation set formed by Equations 30 and 35 encapsulates the meshing condition—with no backlash—of a pair of conical involute gears, each bound to revolve about its own axis. More specifically, Equation 35 involves the geometry of the two beveloid gears, together with the relative placement of the two gear axes and the axial placement of each gear on its own axis. It had already been presented, though in a slightly different form, in Reference 16. On the other hand, by also encompassing the angular position of the two gears, Equation 30 provides information about their phasing. To this author's knowledge, no such equation has ever been published before.

Unconstrained Beveloid Gears in Tight Mesh

As anticipated at the beginning of the previous section, the whole collection of relative rigid-body positions of two tightly meshing beveloid gears can be determined by generalizing the results just found for a conventional beveloid gear set.

Let us consider again a beveloid gear set, composed of two meshing beveloid gears connected to a rigid frame through revolute pairs. If the distance a_0 and angle α_0 between the revolute pair axes, together with the geometry of the two gears—notably their common-normal base angular thicknesses φ_{01} and φ_{02}—comply with Equation 35, then Equation 30 is satisfied by a simple infinity of values for the ordered pair $(\gamma_{01}, \gamma_{02})$, i.e., the mechanism has a simple infinity of configurations.

Now the two mentioned revolute pairs are replaced by cylindrical pairs, which implies that both gears can be displaced along their axes, in addition to being revolved about them. Consequently, the common-normal base angular thickness φ_{0i} of gear G_i, i.e., the base angular thickness on a cross section of gear G_i going through point A_i (Fig. 2), becomes linearly dependent on the axial placement of the gear. With the aid of Figure 5, the ensuing condition can be laid down (See also Eq. 16)

$$\varphi_{0i} = \varphi_i + \left(k_{i,-1} - k_{i,1}\right)\zeta_i \qquad (i = 1,2) \tag{38}$$

In this equation, φ_i is the reference base angular thickness of gear G_i, i.e., the base angular thickness of a tooth of gear G_i at a reference cross section fixed to the gear. Moreover, ζ_i is the displacement of the common-normal cross section, measured from the reference cross section, positive if concordant with the direction of the z-axis of reference frame W_i (a positive ζ_i is shown in Figure 5).

Quantity γ_{0i} is no longer suited to parameterize the angular position of gear G_i. For instance, if $\gamma_{0i} = 0$ and gear G_i is axially displaced, then the base helix of the reference helicoid $\Sigma_{i,1}$ keeps intersecting the minimum distance segment A_1A_2, which means that the gear undergoes a screw motion with respect to the rigid gear-set frame, thus changing its orientation.

Henceforth the angular position of gear G_i will be parameterized by angle γ_i, which is an angle measured on the reference cross section of the gear. Precisely, γ_i is the angle between two lines belonging to the reference cross section of gear G_i—the projection of the minimum distance segment

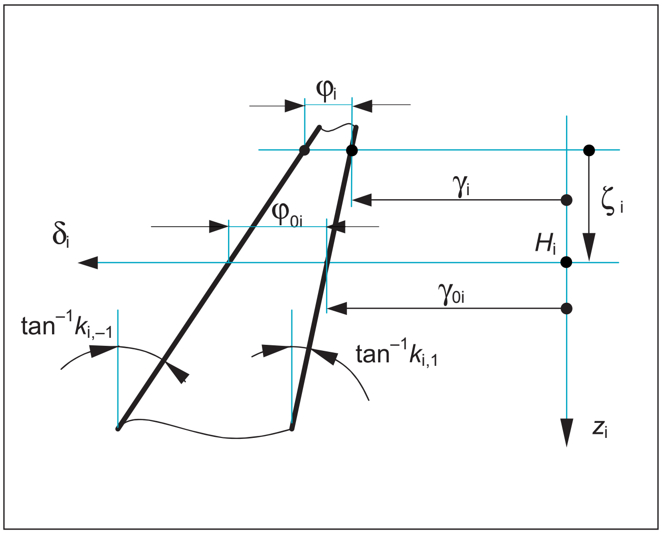

Figure 5—Reference and common-normal parameters.

A_1A_2, and the radial line through the point on the base helix of reference flank $\Sigma_{i,1}$. As shown in Figure 5, the following relation exists between γ_{0i} and γ_i

$$\gamma_{0i} = \gamma_i + k_{i,1}\zeta_i \qquad (i = 1,2) \tag{39}$$

By taking into account Equations 38 and 39, Equations 35 and 30 are transformed into a set of two equations in the four unknowns ζ_1, ζ_2, γ_1 and γ_2. It is generally possible to arbitrarily choose either of γ_i (i=1,2) and either of ζ_i (i=1,2), and then determine the remaining two unknowns. Therefore a set of two beveloid gears connected to the frame by cylindrical pairs has two degrees of freedom, with no need to satisfy any prerequisite similar to Equation 35.

At this point, the frame of the gear set is suppressed altogether, so that parameters a_0 and α_0 are no longer bound to be constant. We are now left with two beveloid gears that can be freely moved in space, provided that they keep meshing with no backlash. All relative rigid-body positions of the two gears are those satisfying Equations 35 and 30, which can be rewritten in the ensuing concise form

$$\begin{cases} U\left(a_0, \alpha_0, \zeta_1, \zeta_2\right) = 0 \\ V\left(a_0, \alpha_0, \zeta_1, \zeta_2, \gamma_1, \gamma_2\right) = 0 \end{cases} \tag{40}$$

In Equation 40, U and V are, respectively, what the left-hand sides of Equations 35 and 30 turn into, once φ_{0i} and γ_{0i} (i=1,2) have been replaced with the expressions provided by Equations 38 and 39.

Equation 40 is a set of two conditions in six unknowns, namely, a_0, α_0, ζ_1, ζ_2, γ_1 and γ_2. Therefore, Equation 40 can be solved in a quadruple infinity of ways, which means that there is a quadruple infinity of possible relative placements for the two beveloid gears.

As explained hereafter, each of these relative placements can be determined by relying on the values of a_0, α_0, ζ_1, ζ_2, γ_1

continued

and γ_2. At first, a skeleton is built based on a_0 and α_0. Such a skeleton is formed by the axes of the two gears, together with the common normal segment A_1A_2 (Fig. 2). Subsequently gear G_i (i= 1,2) is axially placed on its axis by relying on the value of ζ_1. Finally, the orientation of gear G_i about its axis—and with respect to the skeleton segment A_1A_2—is provided by angle γ_i.

Equation 40 will prove pivotal in computing the hobbing parameters of a beveloid gear.

Gear-Hob Relative Movements

As already mentioned at the beginning of the section addressing a backlash-free beveloid gear set, the tooth flanks of a beveloid gear result from a two-parameter envelope by the hob thread flanks. The double-infinite subset of the quadruple infinity of possible gear-hob relative placements is chosen here on the analogy of the hobbing operation of a cylindrical gear by a cylindrical hob. Throughout this section, the generated gear and the enveloping hob will be referred to as gear G_1 and G_2 respectively.

As is known, a cylindrical gear can be hobbed by keeping constant the work-hob axis angle α_0, by revolving the hob about its axis, and by simultaneously moving such an axis across the gear width. In case no hob shift takes place during hobbing—as usually happens—parameter ζ_2 is kept constant too. If the gear and the hob are both cylindrical, it is easy to prove that function U in Equation 40 is deprived of arguments ζ_1 and ζ_2. Therefore, the constancy of the shaft angle α_0 implies the constancy of the axis distance a_0, too; parameters γ_1 and ζ_1 can be thought of as the two parameters of the enveloping process. And for any choice of their values, the second condition in Equation 40 yields quantity γ_2.

Now the hobbing of a beveloid gear by a beveloid hob is analyzed. Similar to the previous case, the shaft angle α_0 is supposed as constant. Its value might be chosen, for instance, with the aim of minimizing the shaft axis distance a_0 at a given cross-section of the gear (see, for instance, Reference 17 for application of this criterion to the hobbing of cylindrical gears). The independent parameters of the envelope are again γ_1 and ζ_1, whereas parameter ζ_2 is kept constant. For any choice of γ_1 and ζ_1, the first and second conditions in Equation 40 yield, respectively, the values of a_0 and γ_2.

The instantaneous movement of the hob relative to the gear being machined can be thought of as the superimposition of two movements:

1. The relative movement of hob and gear as they revolve about their axes (only the independent envelope parameter γ_1 varies)
2. The relative movement of hob and gear when the gear is shifted along its axis without turning with respect to the hobbing machine (only the independent envelope parameter ζ_1 varies)

Since the former movement can be found straightforwardly via Equation 18, only determination of the latter will be pursued here. More specifically, the ensuing ratios of differentials are of interest

$$f_a = \frac{da_0}{d\zeta_1}; \qquad f_\gamma = \frac{d\gamma_2}{d\zeta_1} \tag{41}$$

The differentials on the right-hand sides of Equation 41 are computed with these assumptions

$$\begin{cases} d\alpha_0 = 0 \\ d\zeta_2 = 0 \\ d\gamma_1 = 0 \end{cases} \tag{42}$$

Ratio f_a is the rate of change of the gear-hob axis distance as the hob is moved along the gear width; it is zero for cylindrical gears, but not so for beveloid gears. Ratio f_γ, on the other hand, provides information about the hob rotation as the hob is fed across the work. It would be zero for a spur gear, but is different from zero for helical gears and for most beveloid gears.

To compute ratios f_a and f_γ, Equation 40 is now differentiated by taking into account Equation 42

$$\begin{bmatrix} \dfrac{\partial U}{\partial a_0} & \dfrac{\partial U}{\partial \zeta_1} & 0 \\ \dfrac{\partial V}{\partial a_0} & \dfrac{\partial V}{\partial \zeta_1} & \dfrac{\partial V}{\partial \gamma_2} \end{bmatrix} \begin{bmatrix} da_0 \\ d\zeta_1 \\ d\gamma_2 \end{bmatrix} = 0 \tag{43}$$

Based on Equation 43, the ensuing expression for quantities f_a and f_γ can be obtained

$$f_a = -\frac{\partial U}{\partial \zeta_1}\left(\frac{\partial U}{\partial a_0}\right)^{-1} \tag{44}$$

$$f_\gamma = \left(\frac{\partial U}{\partial \zeta_1}\frac{\partial V}{\partial a_0} - \frac{\partial U}{\partial a_0}\frac{\partial V}{\partial \zeta_1}\right)\left(\frac{\partial U}{\partial a_0}\frac{\partial V}{\partial \gamma_2}\right)^{-1} \tag{45}$$

The partial derivatives in Equations 44 and 45 can be easily computed as shown hereafter. The partial derivative of U with respect to a_0 is given by the ensuing concatenation of relations

$$\frac{\partial U}{\partial a_0} = \frac{\partial S_1}{\partial a_0} + \frac{\partial S_2}{\partial a_0} + \frac{\partial T}{\partial a_0} \tag{46}$$

$$\frac{\partial S_i}{\partial a_0} = N_i\left(k_{i,1}\frac{\partial b_{i,1}}{\partial a_0} - k_{i,-1}\frac{\partial b_{i,-1}}{\partial a_0}\right) \qquad (i = 1,2) \tag{47}$$

$$\frac{\partial T}{\partial a_0} = 2\pi\left(\frac{1}{p_1}\frac{\partial \sigma_1}{\partial a_0} + \frac{1}{p_{-1}}\frac{\partial \sigma_{-1}}{\partial a_0}\right) \tag{48}$$

$$\frac{\partial b_{i,j}}{\partial a_0} = -\lambda_j\frac{v_{i,j} + u_0 v_{h,j}}{v_0\sqrt{Q_j}} \qquad (i = 1,2;\ h = 3-i;\ j = \pm 1) \tag{49}$$

$$\frac{\partial \sigma_j}{\partial a_0} = \lambda_j\frac{v_0}{\sqrt{Q_j}} \qquad (j = \pm 1) \tag{50}$$

As for the partial derivative of U with respect to ζ_1, it is provided by

$$\frac{\partial U}{\partial \zeta_1} = \frac{\partial S_1}{\partial \zeta_1} + \frac{\partial S_2}{\partial \zeta_1} + \frac{\partial T}{\partial \zeta_1} \tag{51}$$

$$\frac{\partial S_1}{\partial \zeta_1} = -N_1 \frac{d\varphi_{01}}{d\zeta_1} = N_1 \left(k_{1,1} - k_{1,-1}\right) \tag{52}$$

$$\frac{\partial S_2}{\partial \zeta_1} = \frac{\partial T}{\partial \zeta_1} = 0 \tag{53}$$

The partial derivative of V with respect to a_0 is given by

$$\frac{\partial V}{\partial a_0} = N_1 k_{1,1} \frac{\partial b_{1,1}}{\partial a_0} + N_2 k_{2,1} \frac{\partial b_{2,1}}{\partial a_0} + \frac{2\pi}{p_1} \frac{\partial \sigma_1}{\partial a_0} \tag{54}$$

The derivatives on the right-hand side of this equation are in turn provided by Equations 49 and 50.

Finally, the partial derivative of V with respect to ζ_1 and γ_2 can be easily determined based on Equations 30 and 39:

$$\frac{\partial V}{\partial \zeta_1} = N_1 k_{1,1} \tag{55}$$

$$\frac{\partial V}{\partial \gamma_2} = N_2 \tag{56}$$

Thanks to Equations 46–55, the ratios f_a and f_γ can be rewritten in the ensuing explicit form:

$$f_a = N_1 v_0 \frac{k_{1,-1} - k_{1,1}}{D_1 - D_{-1}} \tag{57}$$

$$f_\gamma = \frac{N_1}{N_2} \frac{k_{1,1} D_{-1} - k_{1,-1} D_1}{D_1 - D_{-1}} \tag{58}$$

Quantities D_j ($j = \pm 1$) in Equations 57 and 58 are defined by:

$$D_j = \frac{\lambda_j \sqrt{Q_j}}{p_j} \qquad (j = \pm 1) \tag{59}$$

Equations 57–59 show that f_a and f_γ, do not depend on ζ_1, but only on the geometry of gear and hob, together with the swivel angle α_0 (which has been supposed as constant). The constancy of f_a, in particular, explains why the root surface of a beveloid gear is conical—at least if the gear is cut by keeping constant the angle α_0.

Equation 59 provides the expression of D_j ($j = \pm 1$) for any pair of beveloid gears. When gear G_2 is a hob, the number of teeth N_2 is small and the absolute values of the base helix angles $\beta_{2,1}$ and $\beta_{2,-1}$ are relatively large. Therefore the ensuing inequality is generally satisfied

$$a_0 - \rho_{1,j} c_{1,j} - \rho_{2,j} c_{2,j} > 0 \qquad (j = \pm 1) \tag{60}$$

Consequently, Equation 10 reduces to

$$\lambda_j = j \,\mathrm{sign}(v_0) \qquad (j = \pm 1) \tag{61}$$

In addition, since the most commonly used hobs can be considered as involute cylindrical gears rather than beveloid gears, the ensuing additional conditions come into play

$$\begin{cases} p_1 = p_{-1} \\ k_{2,1} = k_{2,-1} \\ v_{2,1} = v_{2,-1} \end{cases} \tag{62}$$

The values of ratios f_a and f_γ, are always needed when programming a CNC hobbing machine that has to cut a beveloid gear. Thanks to Equations 57 and 58, these ratios can be straightforwardly assessed. Therefore, from a utilitarian standpoint, Equations 57 and 58 are the main result of this paper.

Should angle α_0 change while ζ_1 varies (for instance, to constantly minimize the shaft distance a_0), and/or hob shifting occur during machining (for instance, to reduce the scalloping of the tooth flanks of the gear), then the mentioned equations would no longer be applicable. In this occurrence, Equation 40—the true theoretical contribution of this paper—should be resorted to again, and applied afresh to the case at hand.

Numerical Example

The formulae derived in the previous section are here applied to determine quantities f_a and f_γ for the hobbing of a beveloid gear (gear G_1) by a cylindrical hob (gear G_2).

Throughout this section, non-integer quantities are expressed by a high number of digits—all meaningful—in order to allow the reader to accurately check the reported result.

The hob has one thread ($N_2 = 1$) and is characterized by a module of 2 mm and a pressure angle of 20°. Based on this data, the ensuing dimensions can be easily computed

$$\rho_{2,1} = \rho_{2,-1} = 2.735229431127 \text{ mm}$$

$$\beta_{2,1} = \beta_{2,-1} = 69.90659103379 \text{ deg}$$

$$\varphi_2 = 1220.353746100 \text{ deg}$$

The normal base pitches of hob and gear can be derived from the geometry of the hob

$$p_1 = p_{-1} = 5.904262868187 \text{ mm}$$

The gear is characterized by

$$N_1 = 14$$

$$\rho_{1,1} = 13.16838183156 \text{ mm}$$

$$\rho_{1,-1} = 13.15931278723 \text{ mm}$$

$$\beta_{1,1} = -2.515092347823 \text{ deg}$$

$$\beta_{1,-1} = -1.343231785965 \text{ deg}$$

On a given (reference) cross section of the gear, the angular base thickness of the gear teeth is:

$$\varphi_1 = 16.94800000000 \text{ deg}$$

The angle α_0 between the axes of gear and hob is chosen in such a way as to minimize the shaft distance a_0 when point A_1 (Fig. 2) lies on the mentioned reference cross section of the gear. The corresponding values of α_0 and a_0 are:

$$\alpha_0 = -86.03648170877 \text{ deg}$$

$$a_0 = 43.96806431329 \text{ mm}$$

The ratio f_a between the change of axis distance a_0 and the displacement ζ_1 of point A_1 (Figs. 2 and 5) along the gear axis is provided by Equation 57

$$f_a = 0.02988732132842 \text{ mm/mm}$$

On the other hand, the ratio f_γ between the rotation angle of the hob and the displacement ζ_1 of point A_1 along the gear axis—when the gear does not rotate with respect to the hobbing machine—is provided by Equation 58

$$f_\gamma = 2.050765894724 \text{ deg/mm}$$

(To obtain this value, a conversion of unit of measurement has been necessary, since the ratio f_γ yielded by Equation 58 is expressed in radians per unit of length.)

Conclusions

With reference to the generation of a beveloid gear by a hobbing machine, the paper has presented a simple and general method to determine the rate of change of the hob-work axis distance and the differential rotation of the hob as the hob itself is fed across the work. Because it relies on a very few intrinsic dimensions of a beveloid gear, the method is conducive to concise expressions for the desired quantities.

The results presented here refer primarily to the hobbing of a beveloid gear by a beveloid hob, provided that the swivel angle remains constant. On the one hand, they can be readily specialized to the case of a cylindrical hob cutting a beveloid gear. On the other hand, it is easy to extend them to make provision for hob shifting and swivel angle change during hobbing.

References

1. Merritt, H.E. *Gears*, 1954, 3rd Edition, Sir Isaac Pitman & Sons, London.
2. Beam, A.S. "Beveloid Gearing," 1954, *Machine Design*, 26, pp. 36-49.
3. Smith, L.J. "The Involute Helicoid and the Universal Gear," ***Gear Technology***, Nov/Dec., 1990, pp. 18–27.
4. Townsend, D.P. *Dudley's Gear Handbook*, 1991, McGraw-Hill.
5. Mitome, K. "Conical Involute Gear (Part 3—Tooth Action of a Pair of Gears)," *Bulletin of the JSME*, 28, No. 245, pp. 2757–2764.
6. Liu C.-C. and C.-B. Tsay. "Contact Characteristics of Beveloid Gears," 2002, *Mechanism and Machine Theory*, 37, pp. 333–350.
7. Börner, J., K. Humm and F.J. Joachim. "Development of Conical Involute Gears (Beveloids) for Vehicle Transmissions," ***Gear Technology***, Nov./Dec., 2005, pp. 28–35.
8. Liu C.-C. and C.-B. Tsay. "Tooth Undercutting of Beveloid Gears," 2001, *ASME Journal of Mechanical Design*, 123, pp. 569–576.
9. Brauer, J. "Analytical Geometry of Straight Conical Involute Gears," 2002, *Mechanism and Machine Theory*, 37, pp. 127–141.
10. Mitome, K. "Conical Involute Gear—Analysis, Design, Production and Applications," 1981, *Int. Symposium on Gearing & Power Transmissions*, Tokyo, pp. 69–74.
11. Mitome, K. "Table Sliding Taper Hobbing of Conical Gear Using Cylindrical Hob. Part 1—Theoretical Analysis of Table Sliding Taper Hobbing," 1981, A*SME Journal of Engineering for Industry*, 103, pp. 446–451.
12. Mitome, K. "Table Sliding Taper Hobbing of Conical Gear Using Cylindrical Hob. Part 2—Hobbing of Conical Involute Gear," 1981, ASME Journal of Engineering for Industry, 103, pp. 452-455.
13. Mitome, K. "Conical Involute Gear (Part 1—Design and Production System)," 1983, *Bulletin of the JSME*, 26, No. 212, pp. 299–305.
14. Mitome, K. "Inclining Work-Arbor Taper Hobbing of Conical Gear Using Cylindrical Hob," 1986, *ASME Journal of Mechanisms, Transmissions, and Automation in Design*, 108, pp. 135–141.
15. Mitome, K. "A New Type of Master Gears of Hard Gear Finisher Using Conical Involute Gear," 1991, *Proc. of the Eight World Congress on the Theory of Machines and Mechanisms*, Prague, Aug. 26–31, pp. 597–600.
16. Innocenti, C. "Analysis of Meshing of Beveloid Gears," 1997, *Mechanism and Machine Theory*, 32, pp. 363–373.
17. Innocenti, C. "Optimal Choice of the Shaft Angle for Involute Gear Hobbing," 2008, *ASME Journal of Mechanical Design*, 130, pp. 044502.1-044502.5.

Carlo Innocenti *is a professor of Mechanics of Machines at the University of Modena and Reggio Emilia, Italy. After obtaining a degree in mechanical engineering in 1984, he worked for two different companies—as a computation engineer and as a mechanical designer, respectively. He then joined academia in 1990. The papers that he has authored or co-authored are mainly focused on the kinematic analysis and synthesis of planar and spatial mechanisms; rotordynamics; vehicle dynamics; robot calibration; gears and gearing systems.*